

## Involvement of the Pyrophosphate and the 2'-Phosphate Binding Regions of Ferredoxin-NADP<sup>+</sup> Reductase in Coenzyme Specificity\*

Received for publication, July 22, 2003, and in revised form, September 11, 2003  
Published, JBC Papers in Press, September 18, 2003, DOI 10.1074/jbc.M307934200

Jesús Tejero‡, Marta Martínez-Júlvez‡, Tomás Mayoral§, Alejandra Luquita‡¶, Julia Sanz-Aparicio§, Juan A. Hermoso§, John K. Hurley||, Gordon Tollin||, Carlos Gómez-Moreno‡, and Milagros Medina‡\*\*

From the ‡Departamento de Bioquímica y Biología Molecular y Celular, Facultad de Ciencias, Universidad de Zaragoza, 50009 Zaragoza, §Grupo de Cristalografía Macromolecular y Biología Estructural, Instituto Química-Física Rocasolano, Consejo Superior de Investigaciones Científicas Serrano 119, 28006 Madrid, Spain, and the ||Department of Biochemistry and Molecular Biophysics, University of Arizona, Tucson, Arizona 85721

Previous studies indicated that the determinants of coenzyme specificity in ferredoxin-NADP<sup>+</sup> reductase (FNR) from *Anabaena* are situated in the 2'-phosphate (2'-P) NADP<sup>+</sup> binding region, and also suggested that other regions must undergo structural rearrangements of the protein backbone during coenzyme binding. Among the residues involved in such specificity could be those located in regions where interaction with the pyrophosphate group of the coenzyme takes place, namely loops 155–160 and 261–268 in *Anabaena* FNR. In order to learn more about the coenzyme specificity determinants, and to better define the structural basis of coenzyme binding, mutations in the pyrophosphate and 2'-P binding regions of FNR have been introduced. Modification of the pyrophosphate binding region, involving residues Thr-155, Ala-160, and Leu-263, indicates that this region is involved in determining coenzyme specificity and that selected alterations of these positions produce FNR enzymes that are able to bind NAD<sup>+</sup>. Thus, our results suggest that slightly different structural rearrangements of the backbone chain in the pyrophosphate binding region might determine FNR specificity for the coenzyme. Combined mutations at the 2'-P binding region, involving residues Ser-223, Arg-224, Arg-233, and Tyr-235, in combination with the residues mentioned above in the pyrophosphate binding region have also been carried out in an attempt to increase the FNR affinity for NAD<sup>+</sup>/H. However, in most cases the analyzed mutants lost the ability for NADP<sup>+</sup>/H binding and electron transfer, and no major improvements were observed with regard to the efficiency of the reactions with NAD<sup>+</sup>/H. Therefore, our results confirm that determinants for coenzyme specificity in FNR are also situated in the pyrophosphate binding region and not only in the 2'-P binding region. Such observations also suggest that other regions of the protein, yet to be identified, might also be involved in this process.

Although the general catalytic mechanism of many NAD(P)<sup>+</sup>/H-dependent flavoenzymes is known, and despite the fact that the only difference between the two coenzymes is the 2'-P of the NADP<sup>+</sup>/H, the mechanism by which each enzyme is able to recognize either NAD<sup>+</sup>/H or NADP<sup>+</sup>/H is not yet completely understood (1–3). Nevertheless, during the last decade considerable progress has been made in the study of the determinants of coenzyme specificity in different pyridine nucleotide-dependent enzymes with the ultimate goal of shifting such coenzyme specificity via site-specific mutagenesis (2, 4–7).

The flavoenzyme ferredoxin-NADP<sup>+</sup> reductase (FNR)<sup>1</sup> catalyzes the reduction of NADP<sup>+</sup> to NADPH in photosynthesis (3, 8). This reaction is highly specific for NADP<sup>+</sup>/H relative to NAD<sup>+</sup>/H (1, 9). Extensive characterization of FNR from different sources has been reported, with its structural arrangement being the prototype for a family of flavin oxidoreductases that interact specifically with either NADP<sup>+</sup>/H or NAD<sup>+</sup>/H (8, 10–13). Previous studies on *Anabaena* FNR indicated that all of the residues interacting with the 2'-P are not involved to the same extent in determining coenzyme specificity (1). Thus, whereas in *Anabaena* FNR Ser-223 (previous studies on the single S223D mutant) and Tyr-235 (previous studies on the Y235F and Y235A mutants) have been shown to be critical residues in determining NADP<sup>+</sup>/H orientation and specificity, Arg-224 and Arg-233 only provide secondary interactions (1). Moreover, it has also been shown that the determinants for coenzyme specificity are not provided solely by those residues directly interacting with the 2'-P. Thus, in pea FNR, as well as in related flavoenzymes containing an FNR module, it has been shown that a conserved aromatic side chain shields the flavin ring and occupies the putative position of the nicotinamide moiety during ET involving protein substrates. It has been shown that this amino acid in FNR, and in many members of the FNR family, occupies the terminal sequence position and modulates the enzyme NADP<sup>+</sup>/H binding affinity and selectivity (2, 7, 9, 14, 15).

Recent studies (1, 16) also point to other regions of the protein that must undergo specific structural rearrangements of the backbone for proper coenzyme binding, which might contribute to the observed specificity. Sequence and structural analysis of different members of the FNR family with affinity

\* This work was supported by Comisión Interministerial de Ciencia y Tecnología Grants BIO2000-1259 (to C. G.-M.) and BQU2001-2520 (to M. M.), by CONSI+D Grant P006/2000 (to M. M.), and by the National Institutes of Health Grant DK15057 (to G. T.). The costs of publication of this article were defrayed in part by the payment of page charges. This article must therefore be hereby marked "advertisement" in accordance with 18 U.S.C. Section 1734 solely to indicate this fact.

¶ Present address: Cátedra de Física Biológica, Dept. de Ciencias Fisiológicas, Facultad de Ciencias Médicas, Santa Fé 3100, 2000 Rosario, Argentina.

\*\* To whom correspondence should be addressed: Dept. de Bioquímica y Biología Molecular y Celular, Facultad de Ciencias, Universidad de Zaragoza, 50009 Zaragoza, Spain. Tel.: 34 976 762476; Fax: 34 976 762123; E-mail: mmedina@unizar.es.

<sup>1</sup> The abbreviations used are: FNR, ferredoxin-NADP<sup>+</sup> reductase; FNR<sub>ox</sub>, FNR in the oxidized state; FNR<sub>rd</sub>, FNR in the reduced state; FNR<sub>sq</sub>, FNR in the semiquinone state; Fd, ferredoxin; Fd<sub>rd</sub>, Fd in the reduced state; dRf, 5-deazariboflavin; 2'-P, 2'-phosphate; ET, electron transfer; 2'-P-AMP, 2'-phospho-AMP portion of NADP<sup>+</sup>/H; WT, wild type; Mes, 4-morpholineethanesulfonic acid.

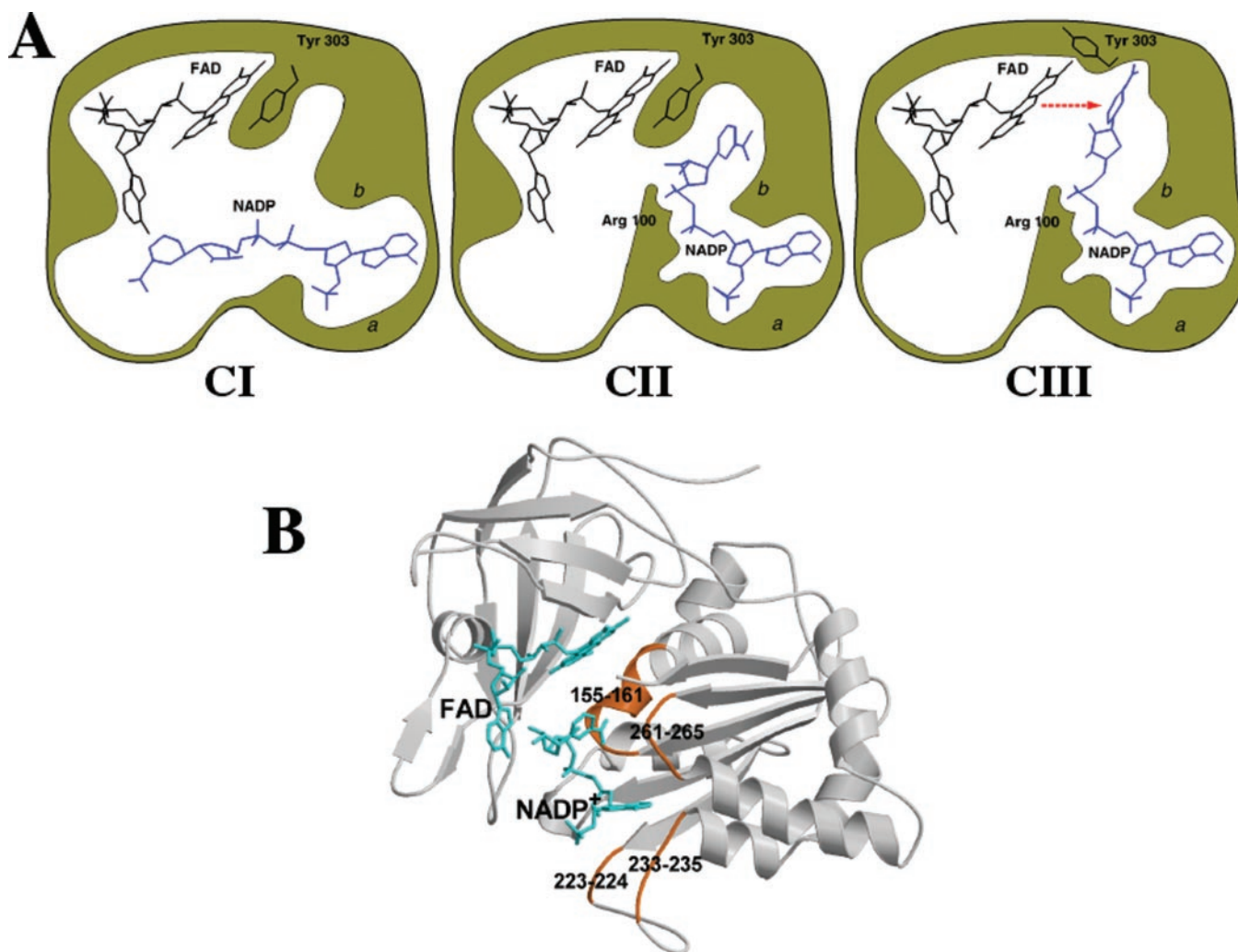


FIG. 1. A, proposed sequence of three steps for the coenzyme recognition and binding mechanism. Initial recognition of NADP<sup>+</sup> through its 2'-P-AMP moiety, which mainly involves region *a* (residues 221–239), is represented by complex CI (left). A structural reorganization of FNR to stabilize the 2'-P-AMP and pyrophosphate moieties follows, leading to complex CII (center). As found in CII, this reorganization involves a conformational change of Arg-100 and movements of regions *a* (see above) and *b* (residues 261–268). Finally, as can be deduced from complex CIII (right), when the C-terminal Tyr moves away from the flavin, the nicotinamide replaces Tyr with its A side facing the re-face of the isoalloxazine central ring in order to allow hydride transfer. B, structure of the *Anabaena* FNR-NADP<sup>+</sup> complex obtained by co-crystallization (16) showing the regions involved in coenzyme specificity (colored in orange). FAD and NADP<sup>+</sup> moieties are drawn in stick representation.

for either NADP<sup>+</sup>/H or NAD<sup>+</sup>/H suggested that the regions formed by residues 155–161 and 261–265 of *Anabaena* FNR might be involved in such conformational changes and, therefore, in coenzyme discrimination (see Fig. 1 and Table I in Ref. 1). Previous studies (1) have shown that replacement by site-directed mutagenesis of the *Anabaena* FNR Thr-155 (a residue present in all NADP<sup>+</sup>/H-dependent members) by Gly (a residue present in all NAD<sup>+</sup>/H-dependent members) produced an increase in the affinity of FNR for NAD<sup>+</sup>/H while producing an important structural modification in the 261–265 loop. Moreover, the structure recently solved for an *Anabaena* FNR-NADP<sup>+</sup> complex shows a conformation for the 261–265 loop more similar to that shown by the corresponding residues of several NAD<sup>+</sup>/H-dependent members of the FNR family than the conformation observed for this loop in free FNR (see Fig. 2 in Ref. 16). In particular, a Pro residue from a “Pro-rich loop” in the NAD<sup>+</sup>/H-dependent enzymes is systematically placed in the uncomplexed enzyme at the same position that the critical Leu-263 residue occupies in the co-crystallized FNR-NADP<sup>+</sup> complex upon NADP<sup>+</sup> binding (Fig. 1A, CII) (16). In addition, structural comparison of the *Anabaena* FNR-NADP<sup>+</sup> complex, obtained after soaking native FNR crystals in an NADP<sup>+</sup> so-

lution (Fig. 1A, CI) (11), with the complex between NADP<sup>+</sup> and a pea FNR mutant in which the C-terminal Tyr residue was replaced by Ser (Fig. 1A, CIII) (13) allows us to postulate a mechanism of coenzyme recognition and binding involving structural reorganization of the enzyme (16) (Fig. 1A). However, these structural rearrangements observed in FNR upon coenzyme binding are already observed in the NAD<sup>+</sup>/H-dependent enzymes in the absence of coenzyme (16). These observations clearly suggest that the mechanisms for coenzyme recognition and complex reorganization in FNR, and therefore in NADP<sup>+</sup>/H-dependent members of the FNR family, are different from those of the NAD<sup>+</sup>/H-dependent enzymes. Thus, in the case of the FNR, it seems that the free enzyme possesses a large cavity to accommodate the 2'-P-AMP moiety of the coenzyme, which upon binding is reorganized in order to perfectly match the charge and shape of the adenine portion of the substrate. However, in the case of the NAD<sup>+</sup>/H-dependent family members, such a narrow cavity is already preformed in the free enzyme and probably does not need to undergo significant structural rearrangements in order to accommodate the adenine moiety of NAD<sup>+</sup>/H, as has been described for the case of the phthalate dioxygenase reductase-NADH complex (16, 17).

Therefore, this cavity formation must contribute to the coenzyme specificity in the FNR family, which might be explained as a consequence of the nature of both the residues interacting directly with the 2'-P and the residues shaping the pocket that accommodates the pyrophosphate moiety. In the present study further site-directed mutagenesis studies have been carried out in these *Anabaena* FNR regions (Fig. 1) in order to clarify the subtle structural features that confer coenzyme specificity. The following groups of mutations on *Anabaena* FNR have been investigated (Fig. 1B): (a) single and combinational mutations in the pyrophosphate binding region involving residues Thr-155, Ala-160, and Leu-263; (b) combinational mutations at the 2'-P binding region involving residues Ser-223, Arg-224, Arg-233, and Tyr-235; and (c) simultaneous mutations at the pyrophosphate and the 2'-P-binding sites. The obtained binding, kinetic, and structural data have been compared with those of WT FNR, and other FNR mutants previously reported, in order to clarify the subtle structural features that confer coenzyme specificity to this enzyme.

#### MATERIALS AND METHODS

**Oligonucleotide-directed Mutagenesis**—*Anabaena* FNR site-directed mutants were prepared by two different methods. Some of the mutants were prepared by using the Transformer site-directed mutagenesis kit (Clontech) in combination with suitable synthetic oligonucleotides (1) and by using as template a construct of the *petH* gene previously cloned into the expression vector pTrc99a (1). A new construct, pET28-FNR, was also prepared by cloning the *petH* gene into the NcoI and HindIII sites of the pET-28a(+) vector (Novagen). The mutants prepared by using this latter construct as template were produced using the QuikChange mutagenesis kit (Stratagene) with suitable oligonucleotides. The pTrc99a vectors with the desired mutation were used to transform the *Escherichia coli* PC strain 0225 (18), whereas the pET28-FNR vectors were transformed into *E. coli* BL21(DE3) Gold cells (Stratagene).

**Purification of *Anabaena* Ferredoxin and FNR Mutants**—FNR mutants from pTrc99a vectors were purified from isopropyl-1-thio- $\beta$ -D-galactopyranoside-induced LB cultures as described previously (18). An analogous protocol was used for mutants of pET28-FNR, but cultures were grown at 30 °C for 24 h, and no isopropyl-1-thio- $\beta$ -D-galactopyranoside was added. Some of the mutants were not retained by the Cibacron blue gel and were purified by using a fast protein liquid chromatography system from Amersham Biosciences with a Mono-Q column (1). Recombinant WT Fd from *Anabaena* was prepared as described (19). UV-visible spectra and SDS-PAGE were used as purity criteria.

**Spectral Analysis**—Ultraviolet/visible spectral analyses were carried out using either a Hewlett-Packard diode array 8452 spectrophotometer, a KONTRON Uvikon 860 spectrophotometer, or a KONTRON Uvikon 942 spectrophotometer. Circular dichroism was carried out on a Jasco 710 spectropolarimeter at room temperature. Far-UV spectra were carried out with either 0.7  $\mu$ M protein in a 1-cm path length cuvette or 5  $\mu$ M protein in a 1-mm path length cuvette. Protein concentrations for the near-UV/visible spectra were between 3 and 5  $\mu$ M in a 1-cm path length cuvette. Photoreduction of different FNR forms was performed at room temperature in an anaerobic cuvette containing 32–65  $\mu$ M FNR samples and 3  $\mu$ M dRf in 50 mM Tris/HCl buffer, pH 8, under anaerobic conditions as described previously (1). Dissociation constants of the complexes between oxidized FNR mutants and either NADP<sup>+</sup> or NAD<sup>+</sup> were measured by difference spectroscopy as described previously (1). Errors in the estimated  $K_d$  values were  $\pm$ 15%.

**Enzymatic Assays**—Diaphorase activity, assayed with 2,6-dichlorophenolindophenol as artificial electron acceptor, was determined for all the FNR mutants in 50 mM Tris/HCl, pH 8.0, as described previously (1). In the case of the diaphorase reactions studied with NADH, high enzyme concentrations (0.5–9  $\mu$ M) were required in order to detect and follow their activity. Therefore, in some of these cases the coenzyme concentration used was only 100 times higher than that of the corresponding enzyme. This was also the case for all FNR forms containing the S223D mutation when using NADPH, where the enzyme concentration in the cuvettes was 4  $\mu$ M. When assaying the reaction of the other FNR enzymes with NADPH, enzyme concentrations in the range 3–500 nM were used. Errors in the estimated values of  $K_m$  and  $k_{cat}$  were  $\pm$ 25 and  $\pm$ 10%, respectively.

**Stopped-flow Kinetic Measurements**—Fast electron transfer (ET) processes between NADPH or NADH and the different FNR<sub>ox</sub> mutants were studied by stopped-flow methodology in 50 mM Tris/HCl, pH 8.0, under anaerobic conditions using an Applied Photophysics SX17.MV spectrophotometer interfaced with an Acorn 5000 computer using the SX18.MV software of Applied Photophysics as described previously (1, 18). The apparent observed rate constants ( $k_{app}$ ) were calculated by fitting the data to a mono- or bi-exponential equation. Errors in their estimated values were  $\pm$ 15%. Final FNR concentrations were kept between 6 and 11  $\mu$ M. Unless otherwise stated final NADPH concentrations were in the range of 160–200  $\mu$ M, whereas NADH was used at  $\sim$ 2.5 mM. The time course of the reactions was followed at 460 nm, although other wavelengths, 340 and 600 nm, were also analyzed.

**Laser Flash Photolysis Measurements**—The laser flash photolysis and the photochemical systems that generate reduced protein *in situ* were as described previously (18, 20, 21). Samples containing 0.1 mM dRf and 1 mM EDTA in 4 mM potassium phosphate buffer, pH 7.0, were deaerated in a long stem 1-cm path length cuvette by bubbling with H<sub>2</sub>O-saturated argon gas for 1 h. Microliter volumes of concentrated protein were introduced through a rubber septum using a Hamilton syringe under anaerobic conditions. Generally, 4–10 flashes were averaged. Kinetic traces were analyzed using a computer fitting routine (Kinfit, OLIS, Bogart, GA). Experiments were performed at room temperature.

**Crystal Growth, Data Collection, and Structure Refinement**—Crystals of the L263P, T155G/A160T, and T155G/A160T/L263P FNR mutants were grown by the hanging drop method. The 5- $\mu$ l droplets consisted of 2  $\mu$ l of 0.75 mM protein solution buffered with 10 mM Tris/HCl, pH 8.0, 1  $\mu$ l of unbuffered  $\beta$ -octyl glucoside at 5% (w/v), and 2  $\mu$ l of reservoir solution containing 18–20% (w/v) polyethylene glycol 6000, 20 mM ammonium sulfate, 0.1 M Mes/NaOH, pH 5.0. The droplets were equilibrated against 1 ml of reservoir solution at 20 °C. Under these conditions crystals grew to a maximum size of 0.8  $\times$  0.4  $\times$  0.4 mm within 1–7 days in the presence of phase separation caused by the detergent. Cryoprotectant additives were tested in order to find suitable conditions to use cryotechniques. Finally, crystals were soaked in a solution containing 70–75% of mother liquor and 25–30% glycerol for 1 min.

One crystal for each FNR mutant was mounted in a fiber loop and frozen at 100 K with a cryogenic system in a nitrogen stream. X-ray data were collected on a Mar Research (Germany) IP area detector using graphite monochromated CuK $\alpha$  radiation generated by an Enraf-Nonius rotating anode generator to a maximum resolution of 1.6 Å. Crystals belong to the P6<sub>3</sub> hexagonal space group. The  $V_m$  is 3.0 Å<sup>3</sup>/Da with one FNR molecule in the asymmetric unit and 60% solvent content. All data sets were processed with MOSFLM (22) and scaled and reduced with SCALA from the CCP4 package (23).

The L263P, T155G/A160T, and T155G/A160T/L263P structures were solved by molecular replacement using the program AmoRe (24) on the basis of the 1.8-Å resolution native FNR model (11) without the FAD cofactor. An unambiguous single solution for the rotation and translation functions was obtained for all proteins. These solutions were refined by the fast rigid body refinement program FITING (25). The models were subjected to alternate cycles of conjugate gradient refinement with the program X-PLOR (26) and manual model building with the software package O (27). Finally, water molecules were added. The resulting model was again subjected to more cycles of positional and  $B$  factor refinement. The final models comprise residues 9–303 (the first 8 residues were not observed in the electron density map), one FAD moiety, one SO<sub>4</sub><sup>2-</sup> molecule, and solvent molecules. Relevant refinement parameters are presented in Table I. The coordinates and structure factors for all these mutants have been deposited in the Protein Data Bank with accession numbers 1OGJ, 1OGI, and 1H42 for the L263P, T155G/A160T, and T155G/A160T/L263P mutants, respectively.

#### RESULTS

**Expression and Purification of the Different FNR Mutants**—The level of expression in *E. coli* of all the mutated FNR forms was judged to be similar to that of the recombinant WT protein. All of the mutants were obtained in homogeneous form and in amounts suitable to perform the demanding characterization studies described herein. FNR forms containing the S223D mutation and also those with more than three mutations in the 2'-P interaction region interacted weakly with the Cibacron blue column (1), thereby requiring the use of a fast protein liquid chromatography Mono-Q column to further purify them.

TABLE I  
 Structure determination statistics

Data collection	FNR form		
	T155G/A160T/L263P	T155G/A160T	L263P
Temperature (K)	100	100	100
X-ray source	Rotating anode	Rotating anode	Rotating anode
Space group	P6 <sub>5</sub>	P6 <sub>5</sub>	P6 <sub>5</sub>
Cell <i>a</i> , <i>b</i> , <i>c</i> (Å)	85.81; 85.81; 96.13	87.32; 87.32; 96.55	87.26; 87.26; 96.69
Resolution range (Å)	31.94–2.15	20.49–1.63	20.49–1.63
No. unique reflections	21,605	50,902	51,351
Completeness of data (%)			
All data	98.9	98.9	99.8
Outer shell	98.9 (2.00–2.15Å)	98.9 (1.73–1.63Å)	99.8 (1.73–1.63Å)
$R_{\text{sym}}^a$	0.095	0.067	0.053
Refinements statistics			
Resolution range (Å)	14.86–2.15	20.5–1.6	19.9–1.6
No. protein atoms	2336	2337	2337
No. hetero atoms	58	58	58
No. solvent atoms	280	358	355
$R_{\text{factor}}^b$ (%)	20.0	20.6	20.7
Free $R_{\text{factor}}^b$ (%)	23.1	22.1	22.8
r.m.s. <sup>c</sup> deviation			
Bond lengths (Å)	0.018	0.010	0.010
Bond angles (degrees)	1.7	1.4	1.4

<sup>a</sup>  $R_{\text{sym}} = \sum_{hkl} \sum_i |I_i - \langle I \rangle| / \sum_{hkl} \sum_i \langle I \rangle$ .

<sup>b</sup>  $R_{\text{factor}} = \frac{\|F_o\| - \|F_c\|}{\|F_o\|} \times 100$ .

<sup>c</sup> r.m.s., root mean square.

**Spectral Properties**—No major differences were detected in the UV-visible absorption or in the near-UV or visible CD spectra of any of the FNR forms (not shown). Therefore, no major structural perturbations appear to have been introduced by the mutations in the FAD environment, and the extinction coefficient of *Anabaena* WT FNR (9.4 mM<sup>-1</sup> cm<sup>-1</sup> at 458 nm) (28) has been assumed herein for all the FNR mutants. The far-UV CD spectra showed only a slight reduction of the 208 nm peak in two mutants, T155G/R224Q/R233L/Y235F and T155G/S223D/R224Q/R233L/Y235F, indicating that only very subtle modifications, if any, have occurred in the protein folding because of the introduced mutations. Illumination of the FNR forms in the presence of dRf caused the reduction of the protein to the neutral FNR semiquinone form (FNR<sub>sq</sub>) with maxima in the range of 588–595 nm for all the FNR mutants. As for the WT enzyme, isosbestic points were also detected around 364 and 507 nm for the oxidized-semiquinone transition for all the mutants. Under the photoreduction conditions only a maximum of 22% of neutral semiquinone results stabilized by WT FNR during the process of full enzyme reduction. A similar amount of semiquinone form was stabilized by most of the mutants, whereas T155G/S223D/R224Q/R233L/Y235F showed an unexpected increase in the proportion of radical stabilized (37%).

**Interaction of FNR Mutants with NADP<sup>+</sup> and NAD<sup>+</sup>**—The interaction of the different FNR forms with either NADP<sup>+</sup> or NAD<sup>+</sup> was investigated by difference spectroscopy. When NADP<sup>+</sup> binds to oxidized WT *Anabaena* FNR, the visible spectrum of the bound flavin undergoes a perturbation, which in the case of the *Anabaena* FNR has been shown to be due to the interaction of the 2',5'-ADP moiety of the cofactor with the reductase (1, 29). In *Anabaena* FNR such spectral perturbations show minima around 392 and 502 nm and maxima around 354, 458, 480, and 522 nm and allowed the estimation of a  $K_d$  value of 5.7 μM (see Fig. 4A in Ref. 1). The spectral perturbations observed for oxidized T155G/A160T FNR upon NADP<sup>+</sup> binding were quite similar in shape to those observed for the WT enzyme, despite a slight displacement of the minima at 392–398 nm, and allowed the determination of the corresponding  $K_d$  value, 21 μM, indicating that binding was 4-fold weaker than that of the WT (Fig. 2, B and C). The

spectral perturbations observed for oxidized L263A and L263P upon NADP<sup>+</sup> binding were similar in shape to those observed for the WT but displaced to longer wavelengths, especially for the L263P FNR mutant that had minima at 396 and 430 nm and maxima around 465 and 492 nm (Fig. 2A). These spectral perturbations allowed the determination of the corresponding  $K_d$  values (Fig. 2C), which were 15 and 40 μM, respectively, for L263A and L263P, indicating that these mutants bind NADP<sup>+</sup> 3- and 7-fold more weakly than the WT FNR. Binding of NADP<sup>+</sup> to the T155G/A160T/L263P FNR form clearly elicited spectral changes at wavelengths different from those for WT FNR, with minima at 396 and 440 nm and maxima around 496 and 512 nm (Fig. 2B), but similar to those previously reported for the T155G FNR mutant (1). Its  $K_d$  value was estimated to be 43 μM, indicating that binding was 7.5-fold weaker than that of the WT. These results suggest that although Leu-263 has more influence in the arrangement of the flavin environment when the coenzyme is bound than Thr-155 and Ala-160, the role played by position 263 is clearly modulated by residues present at positions 155 and 160. When the other oxidized FNR forms were titrated with NADP<sup>+</sup>, only very weak difference spectra were detected in the flavin region for the S223D/R233L/Y235F, R224Q/R233L/Y235F, and S223D/R224Q/R233L/Y235F FNR forms, which barely allowed the estimation of apparently very high values for the dissociation constants. Such results were expected, because it has been shown previously that each one of the individual mutations contained in these multiple mutants affects the ability of FNR to bind NADP<sup>+</sup> (1).

Although NAD<sup>+</sup> was not able to produce any spectral perturbation in the flavin absorption spectrum when added to WT FNR, it has been shown that upon introduction of a Gly residue at Thr-155 of *Anabaena* FNR, NAD<sup>+</sup> titration elicited a weak difference spectrum in the flavin region with maxima at 420 and 505 nm, indicating perturbation of the flavin ring by the coenzyme (see Fig. 4C in Ref. 1). Titration of the L263P and L263A FNR mutants with NAD<sup>+</sup> also elicited difference spectra in the flavin region, but in this case only minima around 390, 455, and 480 nm were observed, suggesting that NAD<sup>+</sup> binds to the flavin environment in a different conformation than it does in the T155G mutant (Fig. 2D). Moreover, titration of the multiple mutants T155G/A160T and T155G/A160T/

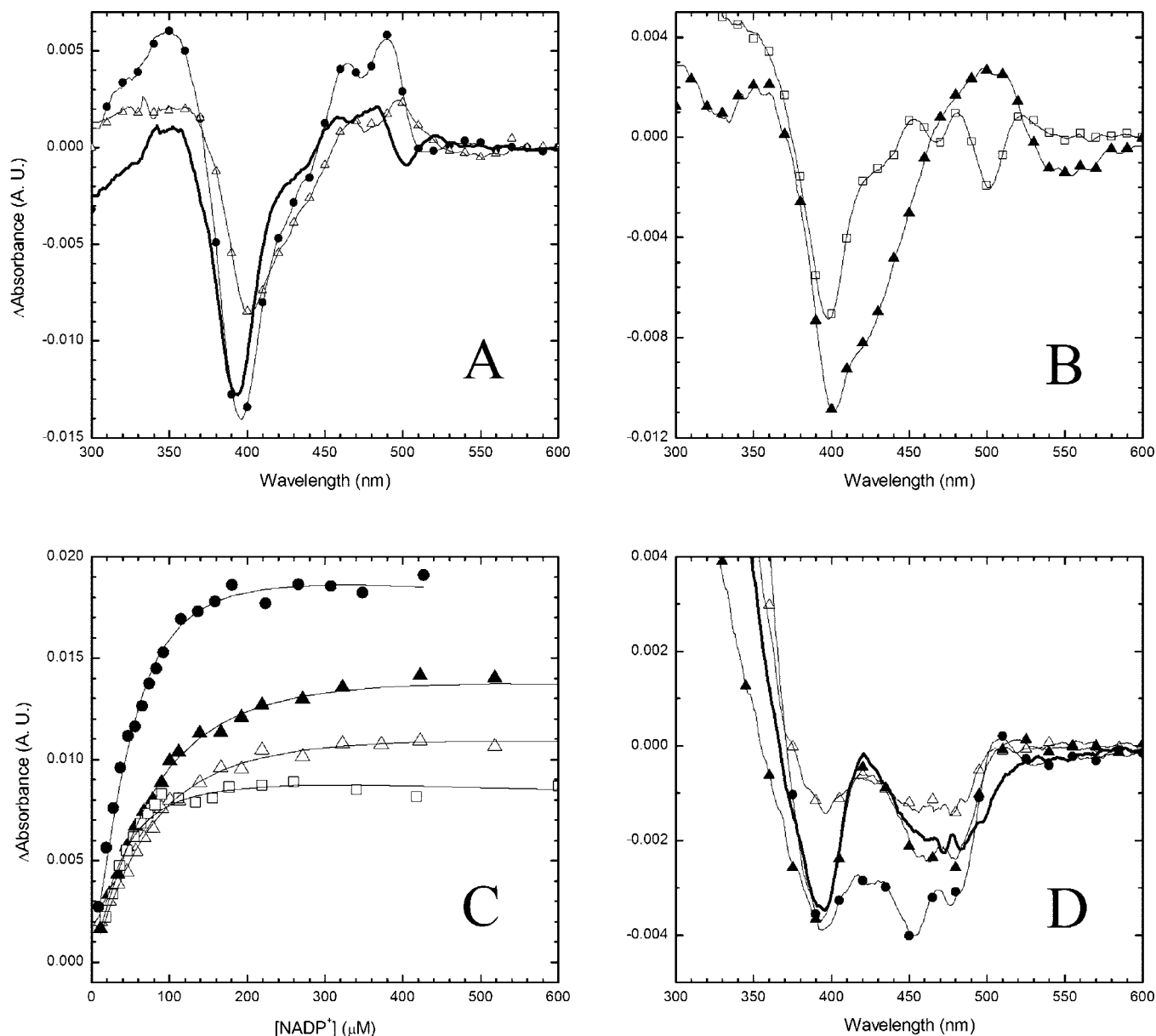


FIG. 2. Spectroscopic characterization of the complexes formed between the FNR<sub>ox</sub> forms and the coenzymes NADP<sup>+</sup> or NAD<sup>+</sup>. A, difference absorbance spectra elicited by binding of WT FNR (solid thick line) (31  $\mu$ M) to NADP<sup>+</sup> (89  $\mu$ M), L263A FNR (closed circles) (56  $\mu$ M) to NADP<sup>+</sup> (353  $\mu$ M), and L263P FNR (open triangles) (54  $\mu$ M) to NADP<sup>+</sup> (700  $\mu$ M). B, difference absorbance spectra elicited by binding of T155G/A160T FNR (open squares) (36  $\mu$ M) to NADP<sup>+</sup> (418  $\mu$ M) and T155G/A160T/L263P FNR (closed triangles) (60  $\mu$ M) to NADP<sup>+</sup> (700  $\mu$ M). C, spectrophotometric titration of selected FNR forms with NADP<sup>+</sup>. L263A FNR (closed circles) (60  $\mu$ M), L263P FNR (open triangles) (61  $\mu$ M), T155G/A160T FNR (open squares) (36  $\mu$ M), and T155G/A160T/L263P FNR (closed triangles) (69  $\mu$ M). D, difference absorbance spectra elicited by the binding of L263A FNR (closed circles) (46  $\mu$ M) to NAD<sup>+</sup> (12.7 mM), L263P FNR (open triangles) (47  $\mu$ M) to NAD<sup>+</sup> (6.9 mM), T155G/A160T FNR (solid thick line) (30  $\mu$ M) to NAD<sup>+</sup> (8.2 mM), and T155G/A160T/L263P FNR (closed triangles) (61  $\mu$ M) to NAD<sup>+</sup> (2.5 mM).

L263P with NAD<sup>+</sup> clearly elicited difference spectra showing the combination patterns described above for the L263P and T155G mutants, with maxima at 420 and 505 nm and minima at 390, 455, and 480 nm (Fig. 2D). Extremely weak difference spectra were also elicited by titration of the R224Q/R233L/Y235F, T155G/R224Q/R233L/Y235F, and T155G/A160T/S223D/R224Q/R233L/Y235F FNR variants with NAD<sup>+</sup>. Moreover, whereas the difference spectra elicited for the R224Q/R233L/Y235F have maxima at 375 and 480 nm, the other two difference spectra have maxima at the same wavelengths as the T155G mutant. Despite the detection of difference spectra, all of the observed perturbations were very weak, and saturation was not reached even at high coenzyme concentration, suggesting very large  $K_d$  values. Nevertheless, these results suggest that upon the introduction of these different mutations confor-

mational modifications at the FNR surface are produced, which allow the positioning of the nicotinamide ring of the NAD<sup>+</sup> close to the flavin ring of FNR. Finally, under the conditions assayed no difference spectra were detected when titrating any of the other FNR forms with NAD<sup>+</sup>.

**Steady-state Kinetics of the Different FNR Forms**—When analyzing the steady-state kinetic parameters of the different FNR mutants for the 2,6-dichlorophenolindophenol-diaphorase reaction using either NADPH or NADH as electron donor (Table II), it was observed that these mutants fall into two categories. One group was formed by those mutants containing any mutation around the FNR 2'-P-binding site (Ser-223, Arg-224, Arg-233, or Tyr-235), whereas the other group contained mutations only at the positions of Thr-155, Ala-160, and Leu-263 (L263A, L263P, T155G/A160T, T155G/A160T/L263P). As ex-

TABLE II  
Steady-state kinetic parameters for the diaphorase activity with 2,6-dichlorophenolindopherol for wild-type and mutated FNR forms from *Anabaena* PCC 7119

FNR forms	$K_m$ NADPH	$k_{cat}$ NADPH	$k_{cat}/K_m$ NADPH	$K_m$ NADH	$k_{cat}$ NADH	$k_{cat}/K_m$ NADH	Specificity for NADPH
	$\mu\text{M}$	$\text{s}^{-1}$	$\text{s}^{-1} \mu\text{M}^{-1}$	$\mu\text{M}$	$\text{s}^{-1}$	$\text{s}^{-1} \mu\text{M}^{-1}$	
WT	6 <sup>a</sup>	81.5 <sup>a</sup>	13.5 <sup>a</sup>	800 <sup>b</sup>	0.16 <sup>b</sup>	$2 \times 10^{-4b}$	67,500
<b>L263P<sup>c</sup></b>	19	17	0.9	650	0.05	$7.7 \times 10^{-5}$	11,688
L263A	15	60	4.0	630	0.13	$2 \times 10^{-4}$	20,000
<b>T155G<sup>b,c</sup></b>	23	97	4.2	178	0.02	$1.1 \times 10^{-4}$	38,181
<b>T155G/A160T<sup>c</sup></b>	22	72	3.3	510	0.07	$1.4 \times 10^{-4}$	23,571
<b>T155G/A160T/L263P<sup>c</sup></b>	12	77	6.4	390	0.33	$8.4 \times 10^{-4}$	7619
R233L/Y235F	1700	22	0.01	2300	0.86	$3.7 \times 10^{-4}$	27
S223D/R233L/Y235F		0.08 <sup>d</sup>		1500	0.10	$6.6 \times 10^{-5}$	
R224Q/R233L/Y235F	3600	1.3	$3.6 \times 10^{-4}$	4300	1.2	$2.7 \times 10^{-4}$	1.4
T155G/R224Q/R233L/Y235F	2700	0.2	$7.4 \times 10^{-5}$	3000	0.28	$9.6 \times 10^{-5}$	0.8
S223D/R224Q/R233L/Y235F		0.05 <sup>d</sup>			0.04 <sup>d</sup>		
T155G/S223D/R224Q/R233L/Y235F		0.06 <sup>d</sup>			0.06 <sup>d</sup>		
T155G/A160T/S223D/R224Q/R233L/Y235F		0.02 <sup>d</sup>			0.04 <sup>d</sup>		
T155G/A160T/S223D/R224Q/R233L/Y235F/L263P	>1800	0.03		12,000	2.1	$1.7 \times 10^{-4}$	

<sup>a</sup> Data from Ref. 18.

<sup>b</sup> Data from Ref. 1.

<sup>c</sup> Mutants with three-dimensional structures solved are highlighted in boldface.

<sup>d</sup> Values for  $k_{cat}$ , which were coenzyme concentration-independent, could only be estimated due to the very small extent of reaction observed.

pected, multiple substitutions in the 2'-P binding region yielded enzymes having greatly reduced catalytic efficiency ( $k_{cat}/K_m$ ) with NADPH (Table II), despite the fact that substitutions around the pyrophosphate binding region (Thr-155, Ala-160, or Leu-263) have also been included. All of these mutants showed significant decreases in their  $k_{cat}$  values with NADPH. This fact allowed only an estimation of  $K_m$  values for some of these mutants, which were very high in some cases (Table II). These mutants had  $k_{cat}$  values for the NADH-dependent reaction that were within a factor of 10 of the value for WT FNR (Table II). Thus, R233L/Y235F, R224Q/R233L/Y235F, T155G/R224Q/R233L/Y235F, and T155G/A160T/S223D/R224Q/R233L/Y235F/L263P show a clear increase of this value (5-, 7-, and 2-fold, respectively), whereas smaller values were obtained for the others. Moreover, when it was possible to estimate  $K_m$  values, these mutants had much higher values for NADH than did WT FNR. Therefore, their catalytic efficiency ( $k_{cat}/K_m$ ) with NADH was within a factor of 10 of the WT FNR value (Table II). Noticeably, in most of these multiple mutants at the 2'-P binding region the catalytic efficiency with NADH is similar to that obtained with NADPH, indicating that the specificity for NADPH had been lost.

Enzymes with single or multiple substitutions at Thr-155, Ala-160, and Leu-263 maintained  $k_{cat}$  values with NADPH and NADH that were comparable with those of the WT FNR (Table II), with the single mutation L263P being the only one having a considerably decreased  $k_{cat}$  value for NADPH.  $K_m$  values for NADPH of this group of mutants showed only moderate increases relative to the WT FNR (2–4-fold), whereas all of them showed only a moderate decrease, within a factor of 2, in the  $K_m$  value for NADH (Table II). Our results also indicate that while the introduction of the single mutation L263P produced an important decrease in the catalytic efficiency with NADPH and a less marked effect with NADH (Table II), replacement of Leu-263 by an Ala produced a more moderate effect. Thus, the L263P mutation decreased the specificity of the enzyme for NADPH versus NADH from a value of 67,500–11,700-fold, whereas the L263A replacement produced an enzyme that is still 20,000 times more specific for NADPH than for NADH (Table II). Combination of the previously characterized T155G mutation (1) with the A160T mutation produced an enzyme that resembles T155G in its behavior, although a further decrease in the specificity for NADPH is observed (Table II). Finally, the triple mutant, T155G/A160T/L263P, showed a be-

havior in which the decreased efficiency with NADPH introduced by the L263P mutation is overcome by the other two introduced mutations. Thus, the enzyme had only half of the catalytic efficiency of the WT with NADPH, whereas this value increased by a factor of 4 with NADH, thereby decreasing the specificity for NADPH versus NADH from 67,500-fold in the WT enzyme to 7,600-fold (Table II).

*Reduction of FNR Mutants Studied by Laser Flash Photolysis*—The reduction of T155G/A160T, T155G/A160T/L263P, T155G/R224Q/R233L/Y235F, and T155G/A160T/S223D/R224Q/R233L/Y235F FNR mutants by laser-generated 5-deazariboflavin (dRfH) was monitored by the absorbance increase at 600 nm, due to FNR<sub>sq</sub> formation. Transients were fit by monoexponential curves, and the obtained rate constants were within a factor of 1.5 that of the WT FNR protein (not shown), indicating that the FAD of all the mutants is accessible and redox-active.

The dependences of  $k_{obs}$  (where  $k_{obs}$  is the pseudo first-order rate constant) on FNR concentration for the Fd<sub>rd</sub>-FNR<sub>ox</sub> electron-transfer interaction at 100 mM ionic strength for the WT FNR and for the T155G/A160T, T155G/A160T/L263P, T155G/R224Q/R233L/Y235F and T155G/A160T/S223D/R224Q/R233L/Y235F FNR mutants are shown in Fig. 3, A and B. The results for the T155G/A160T/L263P and T155G/R224Q/R233L/Y235F mutants and WT FNR are essentially identical (Fig. 3A). The *solid line* through the data in Fig. 3A is a fit of the WT data to the exact solution to the differential equation describing the minimal two-step mechanism of complex formation followed by ET (30, 31) from Fd<sub>rd</sub> to FNR<sub>ox</sub>. This fit yields kinetic parameters of 23  $\mu\text{M}$  for the  $K_d$  value of the intermediate ET complex (Fd<sub>rd</sub>·FNR<sub>ox</sub>) and 6,300  $\text{s}^{-1}$  for  $k_{et}$  (where  $k_{et}$  is the first-order rate electron transfer constant). The T155G/A160T and T155G/A160T/S223D/R224Q/R233L/Y235F mutants (Fig. 3B) are only slightly different. The *solid line* through the data in Fig. 3B is the corresponding fit through the combined data of the two mutants, which yields values of 12  $\mu\text{M}$  for the  $K_d$  value of the intermediate ET complex and 5,500  $\text{s}^{-1}$  for  $k_{et}$ . Note that these data have not been corrected for the presence of preformed complex (20). We have shown previously that this correction has insignificant effects on  $k_{et}$  but does significantly decrease the  $K_d$  values without changing their relative values.

Fig. 4, A and B, shows the dependences of  $k_{obs}$  on ionic strength. It is clearly evident that all the FNR forms analyzed, with only minor variations, react essentially identically to WT FNR. In summary, our data indicate that the Fd-FNR interac-

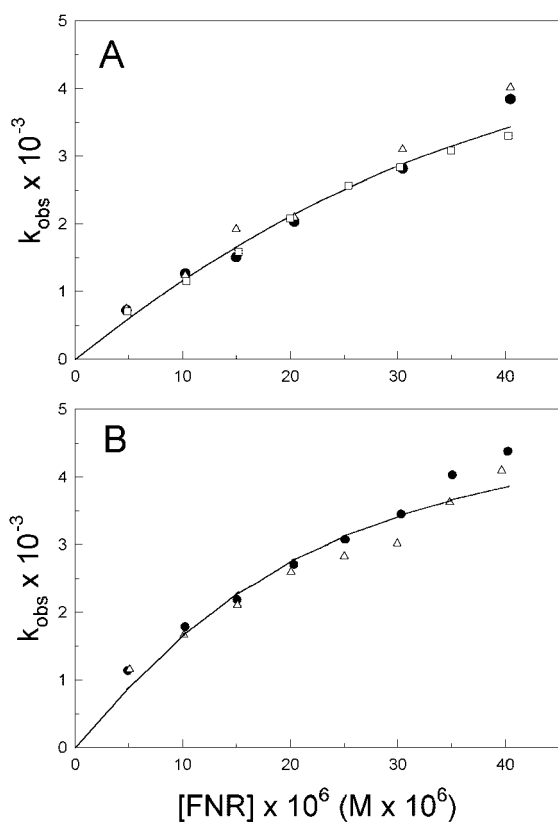


FIG. 3. A, FNR concentration dependence for the reduction of WT (filled circles), T155G/A160T/L263P (open triangles), and T155G/R224Q/R233L/Y235F (open squares) FNR species by  $Fd_{red}$  at 100 mM ionic strength. B, FNR concentration dependence for the reduction of T155G/A160T (filled circles) and T155G/A160T/S223D/R224Q/R233L/Y235F (open triangles) FNR species by  $Fd_{red}$  at 100 mM ionic strength. Solid lines through the data represent theoretical fits assuming a two-step mechanism (see text for details). Fitted data are almost superimposable, and only one fit is shown in each panel (see text for details).

tion and ET are not affected by the introduction of any of the mutations analyzed herein.

**Fast Kinetic Studies of the Reduction of FNR Mutants by NADPH and NADH**—The fast kinetic reaction of the different oxidized *Anabaena* FNR mutants with either NADPH or NADH was determined using stopped-flow methods by following the flavin spectral changes at 460 and 600 nm under anaerobic conditions. The results obtained have been compared with those reported for WT FNR (1, 18). The kinetic traces of the reactions of the L263A, T155G/A160T, and T155G/A160T/L263P FNR forms with NADPH at 460 nm (Fig. 5A) represent two processes that have  $k_{app}$  values which in some cases are up to 3-fold smaller with respect to the reaction of the WT enzyme (Table III). These can be attributed to the production of the charge-transfer complex  $[FNR_{ox}-NADPH]$  (fast process) followed by the hydride transfer from NADPH to FAD (slower process), resulting in the equilibrium mixture of both charge-transfer complexes,  $[FNR_{ox}-NADPH]$  and  $[FNR_{red}-NADPH^+]$ , as reported for the WT enzyme reaction (32). Noticeably, although two processes also take place when the reduction of L263P FNR by NADPH is analyzed, a considerably larger decrease in the  $k_{app}$  values for both processes was observed than that obtained for the L263A mutant relative to WT FNR. Much longer time scales were also required to follow the reaction at 460 nm of NADPH with any of the mutants having multiple mutations at the 2'-P NADPH-binding site (Fig. 5A, inset). Moreover, in most of the cases the observed kinetic traces were best fit to

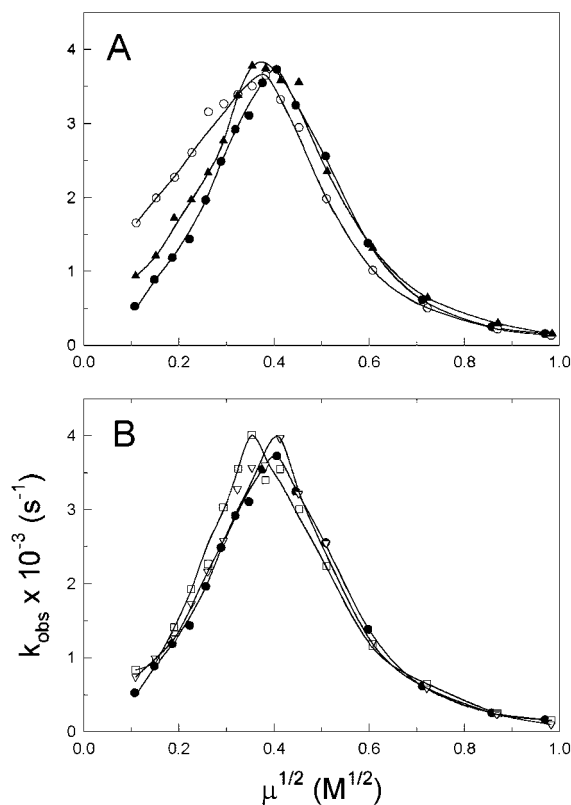


FIG. 4. Ionic strength dependence of  $k_{obs}$  for the reduction of WT (closed circles), T155G/A160T (open circles), T155G/R224Q/R233L/Y235F (closed triangles) (A) and T155G/A160T/S223D/R224Q/R233L/Y235F (open squares) and T155G/A160T/S223D/R224Q/R233L/Y235F (upside-down open triangles) FNR forms by  $Fd_{red}$  (B). Ionic strength was adjusted using aliquots of 5 M NaCl. Deaerated solutions also contained 95–100  $\mu$ M dRF and 1 mM EDTA in 4 mM potassium phosphate buffer, pH 7.0.

mono-exponential processes having  $k_{app}$  values that are 70-fold (R233L/Y235F) to  $1.7 \times 10^6$ -fold (T155G/A160T/S223D/R224Q/R233L/Y235F) smaller than those of the WT enzyme (Table III). Taking into account either the very weak or lack of interaction shown above by difference spectroscopy for these FNR mutants with  $NADP^+$ , the rate of the subsequent ET reaction cannot be estimated due to the slow binding of  $NADP^+$ . Measurements for some mutants were also carried out at 340 and 600 nm (not shown). It is noteworthy that for some of the mutants much slower processes having similar amplitudes and time scales were observed at these wavelengths than those observed at 460 nm. Similar observations were also reported when some individual mutations were analyzed in a previous study (1), and although we do not have an explanation for this at the moment, further work is being done in order to understand this behavior.

Following the reaction of NADH with the different FNR forms investigated herein, most of them showed  $k_{app}$  values that were within a factor of 2 of that of the WT enzyme (Table III and Fig. 5B). However, although some of the reactions were best fit to a mono-exponential process, two processes were detected for many of them, as was also observed for the WT reaction. Moreover, the reactions of NADH with either the L263P or the T155G/A160T/S223D/R224Q/R233L/Y235F FNR forms were 8- and 12-fold, respectively, slower than that of the WT, whereas reduction of R224Q/R233L/Y235F appeared to have a  $k_{app}$  that is slightly faster (4-fold) (Table III). As noted previously in other studies, a very small lag phase can also be observed for some of the mutants. These processes were also

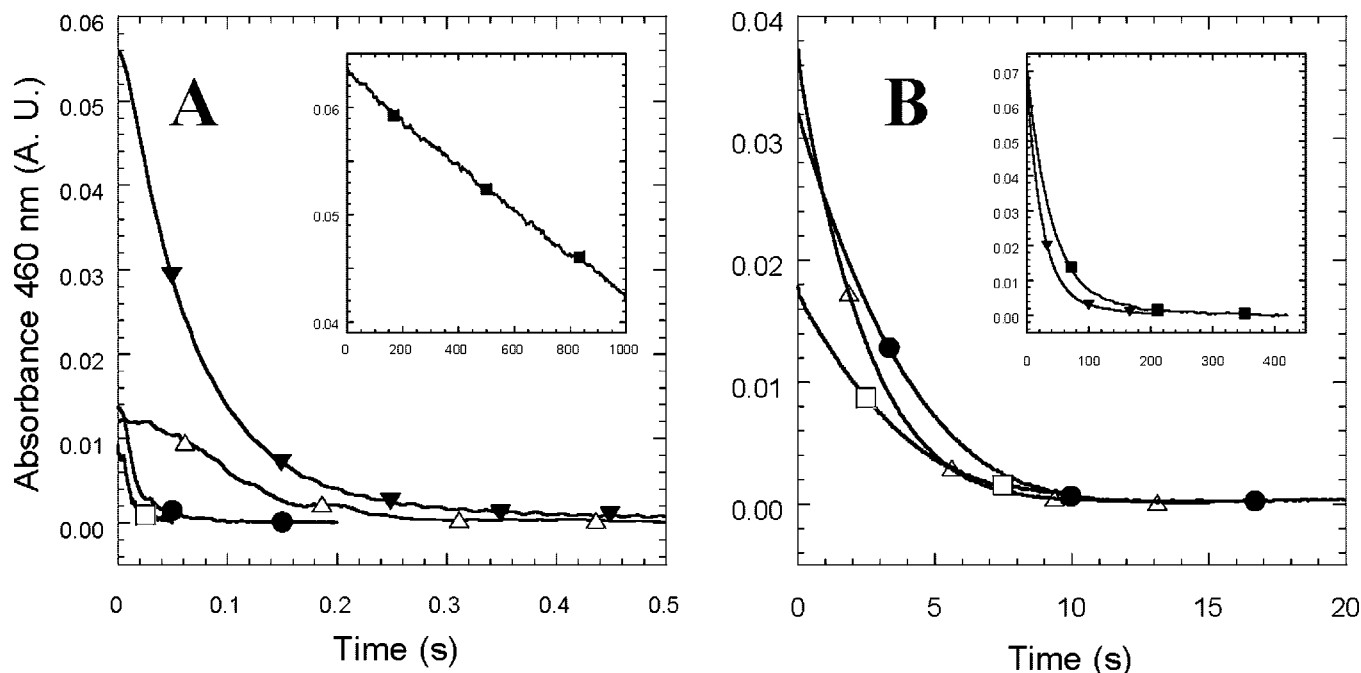


FIG. 5. Time course of the anaerobic reactions of the different FNR forms. A, reactions with NADPH: 8.2  $\mu\text{M}$  T155G/A160T FNR<sub>ox</sub> (open squares) reacted with 170  $\mu\text{M}$  NADPH; 8.7  $\mu\text{M}$  L263A FNR<sub>ox</sub> (closed circles) reacted with 156  $\mu\text{M}$  NADPH; 9.1  $\mu\text{M}$  T155G/A160T/L263P FNR<sub>ox</sub> (open triangles) reacted with 170  $\mu\text{M}$  NADPH; and 9.1  $\mu\text{M}$  L263P FNR<sub>ox</sub> (upside-down closed triangles) reacted with 160  $\mu\text{M}$  NADPH. Inset, 9.4  $\mu\text{M}$  T155G/A160T/S223D/R224Q/R233L/Y235F FNR<sub>ox</sub> (closed squares) reacted with 2.0 mM NADPH. B, reactions with NADH: 8.2  $\mu\text{M}$  T155G/A160T FNR<sub>ox</sub> (open squares) reacted with 2.5 mM NADH; 9.1  $\mu\text{M}$  T155G/A160T/L263P FNR<sub>ox</sub> (open triangles) reacted with 2.2 mM NADH; 9.6  $\mu\text{M}$  L263A FNR<sub>ox</sub> (closed circles) reacted with 2.2 mM NADH. Inset, 9.1  $\mu\text{M}$  L263P FNR<sub>ox</sub> (upside-down closed triangles) reacted with 2.4 mM NADH; 11.7  $\mu\text{M}$  T155G/A160T/S223D/R224Q/R233L/Y235F FNR<sub>ox</sub> (closed squares) reacted with 2.3 mM NADH. Reactions were followed at 460 nm and carried out in 50 mM Tris/HCl, pH 8.0, at 25 °C. Final concentrations are given.

TABLE III

Fast kinetic parameters for the reduction of the different *Anabaena* PCC 7119 FNR forms by NADPH and NADH as obtained by stopped flow

All the reactions were carried out in 50 mM Tris/HCl, pH 8.0, at 25 °C and followed at 460 nm. The samples were mixed in the stopped-flow spectrometer at a final concentration of 6–11  $\mu\text{M}$  for the FNR samples and 160–200  $\mu\text{M}$  for NADPH or 2.5 mM for NADH.

FNR forms	NADPH		NADH	
	$k_{\text{app1}}$	$k_{\text{app2}}$	$k_{\text{app1}}$	$k_{\text{app2}}$
	$s^{-1}$		$s^{-1}$	
WT <sup>a</sup>	>500	200	0.35	0.005
L263P	16	3	0.04	
L263A	115	22	0.32	
T155G <sup>a</sup>	>400	80	0.08	0.012
T155G/A160T	180	60	0.28	
T155G/A160T/L263P	>400	130	0.43	
R233L/Y235F	7.3		0.6	
S223D/R233L/Y235F	0.15		0.2	0.03
R224Q/R233L/Y235F	0.44	0.1	1.5	
T155G/R224Q/R233L/Y235F	0.16	0.015	0.3	0.08
S223D/R224Q/R233L/Y235F	0.07 <sup>b</sup>		0.5	0.02
T155G/S223D/R224Q/R233L/Y235F	2.1 <sup>b</sup>		0.1	0.001
T155G/A160T/S223D/R224Q/R233L/Y235F	0.0003 <sup>b</sup>		0.03	0.001
T155G/A160T/S223D/R224Q/R233L/Y235F/L263P	0.0003 <sup>b</sup>		0.52	

<sup>a</sup> Data from Ref. 1.

<sup>b</sup> Reactions studied with NADPH at a final concentration of 2.5 mM.

analyzed at 600 nm, where all the mutants showed an increase in absorbance followed by a decay ending above the initial baseline. In most of the cases, the first process is consistent with that observed at 460 nm. Thus far, as with the reactions with NADPH at long time scales, we do not have a good explanation for all of the observed processes, and further work is presently underway that should help to elucidate this behavior.

**Three-dimensional Structure of Selected FNR Mutants**—The three-dimensional structures of the L263P, T155G/A160T, and T155G/A160T/L263P FNR mutants have been determined by x-ray diffraction. The first eight residues in the sequence were

not included in all the models due to the poor electron density map in this region; on the contrary, the electron density in the rest of the molecule was of very high quality for the three FNR mutants. Their overall folding showed no significant differences with respect to the native structure, as shown by the very low root mean square deviations of the C $\alpha$  backbone of the mutant superimposed on the native FNR backbone (0.21, 0.28, and 0.31 Å for the L263P, T155G/A160T, and T155G/A160T/L263P FNR mutants, respectively). Only slight differences were observed in the loop starting at Tyr-104 and ending at Val-113, near the region interacting with the adenine moiety of

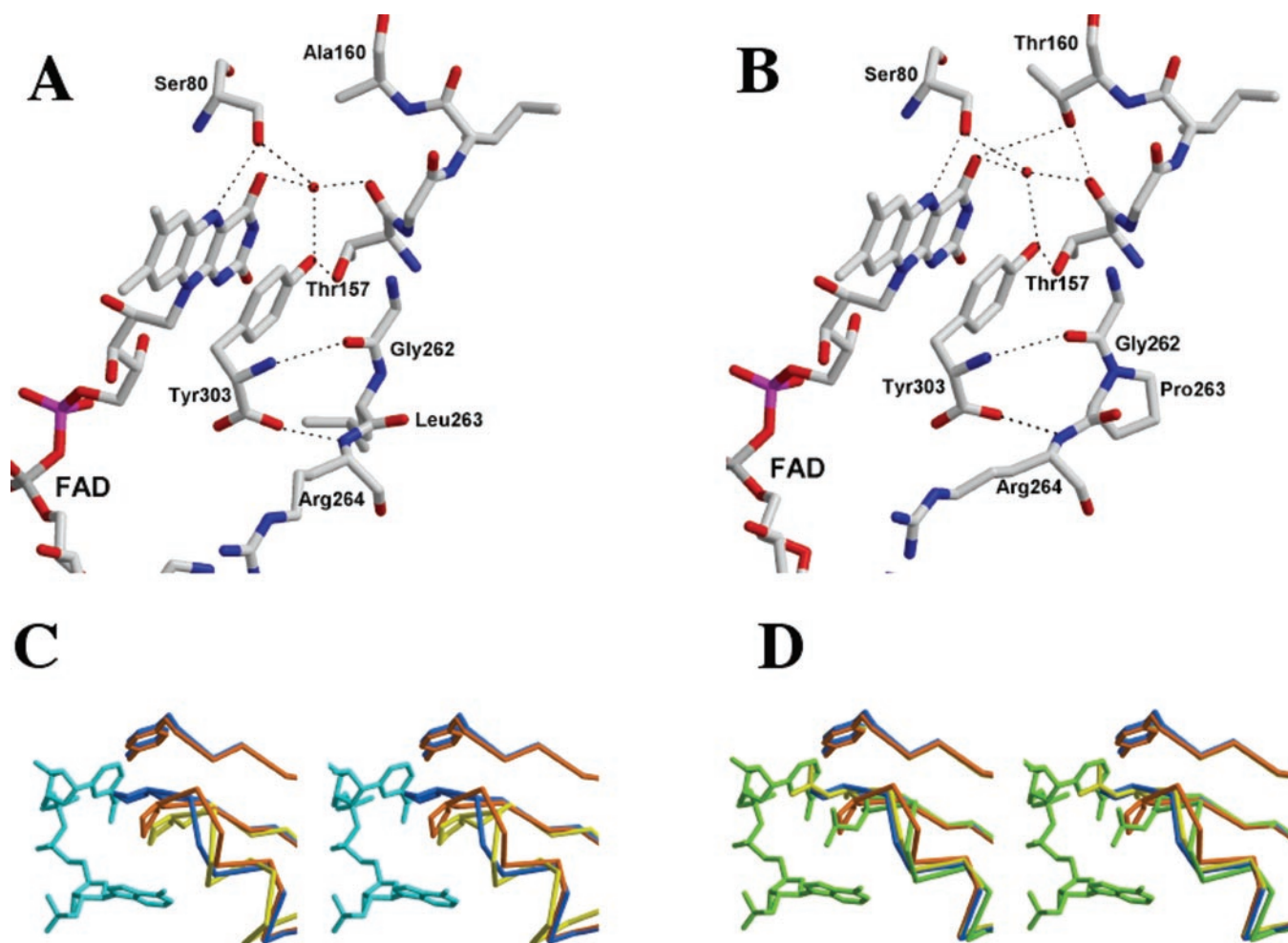


**FIG. 6. Hydrogen bond pattern changes in the FAD environment after mutation at position 160.** *A*, FNR wild type; *B*, T155G/A160T/L263P FNR mutant. Two new interactions are created between Thr-160 and FAD and Thr-157. This pattern is also maintained in the T155G/A160T FNR mutant. *C*, retraction of the 261–265 loop after site-directed mutagenesis. The C $\alpha$  backbone of the 261–265 region is depicted with the Pro-263 residue drawn in a stick representation. Relative position of NADP<sup>+</sup> according to the crystallographic data is shown in light blue stick representation. The L263P FNR mutant is colored in dark blue. This mutant shows a conformation for this region similar to that observed in the WT enzyme. However, a pronounced retraction is observed for this loop in the T155G/A160T/L263P FNR mutant (colored in orange), moving the structure in this region closer to that presented for the NAD<sup>+</sup>/H-dependent nitrate reductase (colored in yellow). *D*, relative position of Leu-263 in the WT FNR (yellow), in the FNR-NADP<sup>+</sup> co-crystallized complex (green) with regard to Pro-263 in the L263P FNR mutant (dark blue), and in the T155G/A160T/L263P FNR mutant (orange). *C* and *D*, the relative position of the C-terminal Tyr-303 (top of the figures) to the analyzed loop is shown.

FAD, but they are not significant due to the high flexibility exhibited for this region in all FNR forms. Concerning the L263P FNR mutant, no structural changes at the mutated position were observed. In this case, the 261–265 loop is in a similar position to that found for the WT enzyme and is not mimicking the conformation of the equivalent Pro-rich region present in the NAD<sup>+</sup>/H members. The absence of conformational changes in this region must be certainly due to steric interference of the introduced Pro residue with the Thr-155 side chain. It has been reported that the retracted conformation of such a Pro-rich region in the NAD<sup>+</sup>/H members would not be compatible with the presence of a Thr (or Pro) at the position 155 (*Anabaena* FNR numbering) in the NADP<sup>+</sup>/H members (1). Surprisingly, in the case of the T155G/A160T FNR mutant, there was not a retraction of the 261–265 loop similar to that observed in the T155G mutant (1). However, a deeper look into the T155G/A160T mutant structure revealed that small but significant changes in the C $\alpha$  backbone of the NADP<sup>+</sup> binding domain (maximal of 0.4 Å) were produced after mutation at position 160. The insertion of a larger side chain (Thr instead of Ala) induced a small displacement of all the strands of the

$\beta$ -sheet in the NADP<sup>+</sup> binding domain. Also a new interaction pattern was created around position 160 (Fig. 6, *A* and *B*): a bifurcated H-bond between the Thr-160 OH side chain and both carbonyl groups of Thr-157 (2.73 Å) and the O-4 group of the FAD (3.58 Å). Remarkably, this protein-cofactor interaction is also present in all the reported structures of the NAD<sup>+</sup>/H-dependent enzymes belonging to the FNR family. Finally, when all three positions were mutated simultaneously (T155G/A160T/L263P), the structure of the FNR mutant showed a displacement of the  $\beta$ -sheet in the NADP<sup>+</sup> binding domain similar to that observed in the T155G/A160T mutant, and more importantly a marked retraction of the 261–265 loop was produced. As observed (Fig. 6*C*), the conformation adopted by this region approaches that exhibited for NAD<sup>+</sup>/H-dependent enzymes. However, Pro-263 in the T155G/A160T/L263P FNR mutant is not situated at the same position as in the NAD<sup>+</sup>/H-dependent enzymes. That could be related to sequence differences between NADP<sup>+</sup>/H- and NAD<sup>+</sup>/H-dependent enzymes. Thus, whereas a Pro residue is present at position 264 in most of the NAD<sup>+</sup>/H-dependent enzymes, an Arg residue occupies this position in FNR. Its backbone N atom forms a strong H-bond

interaction (2.4 Å) with one of the oxygens of the carboxylic moiety of the well stabilized Tyr-303 (see Fig. 6), thereby preventing a more pronounced retraction of the 261–265 loop. It is worth noting that in the WT enzyme this H-bond interaction was broken only after formation of the FNR-NADP<sup>+</sup> complex (16).

Finally, L263P and T155G/A160T also show subtle changes in their cofactor structures compared with WT FNR FAD. Thus, a water molecule was lost in the vicinity of adenine, not allowing its stabilization by the apoprotein portion through a network of water molecules as occurred in WT FNR. This change produced a slight displacement of ribose and adenine moieties of FAD. The new position of adenine was situated 1.03 Å from its conformation in the WT enzyme, being closer to the loop comprising residues 104–113, where interactions between FAD and FNR were conserved. Moreover, the FAD cofactor of the T155G/A160T/L263P FNR mutant showed two different conformations of the ribose and the adenine moieties. One of them was situated similar to that in the L263P and T155G/A160T FNR mutants, whereas the adenine of the other one was rotated 180° and was coplanar with the ring of the Tyr-303 residue.

#### DISCUSSION

Laser flash photolysis studies indicate that the Fd-FNR interaction and ET are not affected by the introduction of any of the mutations analyzed in this study. This confirms that the FNR surface formed by these residues is not occupied by Fd upon complex formation. Such observation favors the geometries proposed for the structure of the putative Fd-FNR-NADP<sup>+</sup> ternary complexes that have been modeled thus far (3, 16). Both models show that the NADP<sup>+</sup>-binding site on FNR is not close to the Fd-FNR interface, and therefore, NADP<sup>+</sup> binding to either WT or any of the FNR mutants here analyzed should not affect the interaction between the two proteins. Moreover, upon NADP<sup>+</sup> binding to WT FNR, structural rearrangements in the 261–265 loop of FNR are observed that involve changes in the conformation and orientation of Arg-264, which moves in such a way that a new ion pair could be formed with Fd (16). This new link might explain why the affinity of Fd is different for the preformed WT FNR-NADP<sup>+</sup> complex than for the free enzyme. However, such a possibility might not apply in the case of the interaction of the different FNR mutants here analyzed with either NADP<sup>+</sup> or NAD<sup>+</sup>, because, in our opinion, the conformational changes that facilitate ET between Fd and FNR must only be produced upon a tight and specific coenzyme-enzyme interaction.

*Effect of Mutations at the Pyrophosphate Interaction Site of NADP<sup>+</sup>*—Previous studies, in which the Thr side chain of residue 155 in *Anabaena* FNR was replaced by a Gly (the residue present in the NAD<sup>+</sup>/H-dependent members of the FNR family), indicated that regions 155–160 and 261–268 of the protein might be involved in determining coenzyme specificity (1). In the present study the behavior of L263P, L263A, T155G/A160T, and T155G/A160T/L263P FNR mutants has been investigated and compared with those of T155G and WT FNRs. With L263A being the only exception, all of these mutants have been produced by replacement of the FNR residues by those residues present at the equivalent positions in NAD<sup>+</sup>/H-dependent members of the FNR family (see Table I in Ref. 1). Remarkably, all these FNR mutants show an important increase in its affinity for NAD<sup>+</sup>/H. This is indicated by the decreases observed in their  $K_m$  values for NADH relative to the WT and by the fact that although no difference spectrum is elicited by WT FNR, all of these mutants elicited difference spectra upon NAD<sup>+</sup> binding (Fig. 2). Moreover, by taking into account these difference spectra, two different binding modes

to FNR seem to be produced: one involving L263P and L263A and the other involving T155G/A160T and T155G/A160T/L263P, with the latter mutant exhibiting combination patterns of the L263P mutant and that reported previously for the T155G (1). However, despite their ability for NAD<sup>+</sup>/H binding, none of these mutants has an enhanced reactivity with NADH, as shown by the very small values obtained for  $k_{cat}$  and  $k_{app}$  when studied by steady-state and by fast kinetic methods. On the other hand, their reactivity with NADPH is only slightly hindered for most of them, with only a noticeably small decrease in ability to accept electrons from NADPH in the case of the L263P FNR form (Tables II and III). Moreover, the efficiency of NADP<sup>+</sup>/H binding does not appear to be hindered in any of them, and different spectroscopic studies again indicate that whereas L263P and L263A bind NADP<sup>+</sup> in a manner similar to WT FNR, T155G/A160T and T155G/A160T/L263P also resemble the T155G FNR mutant in the changes induced upon NADP<sup>+</sup> binding (1). Therefore, our data indicate the structural modifications induced by the introduced mutations enhance the enzyme affinity for NAD<sup>+</sup>/H, whereas they only slightly modulate the FNR affinity for NADP<sup>+</sup>/H. Nevertheless, the complexes formed with NAD<sup>+</sup>/H might not provide an adequate orientation for ET. Moreover, our data also indicate that these mutants, particularly L263P, accommodate the NADP<sup>+</sup>/H coenzyme in a different orientation with regard to the flavin ring than does the WT FNR.

*The Structure Explains the Different Interaction of the Coenzyme with the L263P and the T155G/A160T/L263P Mutants*—Analysis of the L263P, T155G/A160T, and T155G/A160T/L263P FNR three-dimensional structures indicates that the introduced mutations produced different effects depending on their combinations (Fig. 6C), which influence a slight displacement of the backbone of the enzyme along these regions of the NADP<sup>+</sup> binding domain. In particular, important structural differences are observed in the loop comprising residues 261–265 among these mutants (Fig. 6C). Thus, the three-dimensional position of Pro at position 263 differs noticeably depending on the FNR form. In the case of the L263P FNR form, this Pro is pointing to the position occupied by the Leu-263 in the free enzyme, whereas in the case of the T155G/A160T/L263P FNR mutant, Pro-263 is situated near the position occupied by Leu-263 when NADP<sup>+</sup> is bound (13, 16) (see Fig. 6D). As mentioned previously, this different rearrangement of the 261–265 loop is mainly related to both the Pro composition of the 261–265 loop and to the propensity of the amino acid composition of the 155–161 region to be compatible with the new conformation. In this sense, a Pro-rich region involves a tighter conformation for the 261–265 loop if residues in the 155–161 region do not interfere with it. In particular, a Gly residue at position 155 seems to be crucial to allow this retracted conformation of the Pro-rich loop in the NAD<sup>+</sup>/H-dependent members. Besides, a Thr residue at position 160 also seems to be specific for the NAD<sup>+</sup>/H-dependent enzymes, which mainly produce a different organization of the hydrogen bond network (including a new interaction with the FAD cofactor that is not present in the NADP<sup>+</sup>/H-dependent members) and a small movement of the  $\beta$ -sheet around the cofactor. Additional differences in the hydrogen bond network can be deduced from the structural comparison of the NADP<sup>+</sup>/H- and NAD<sup>+</sup>/H-dependent members of the FNR family. Thus, whereas a strong interaction between the Tyr terminal residue and the 261–265 loop (more specifically with the backbone N atom of the residue at position 264) occurs in the NADP<sup>+</sup>/H-dependent members, this interaction does not exist in the NAD<sup>+</sup>/H-dependent members as this position is occupied by another Pro residue. Interestingly, FNR has lost this interaction upon NADP<sup>+</sup> binding (16).

Therefore, this feature also seems to be also important because, as deduced from the structure of the T155G/A160T/L263P FNR mutant, the presence of the above-mentioned strong interaction reduces the effect of the 261–265 loop retraction.

Therefore, all these facts indicate that the simultaneous replacement of Thr-155, Ala-160, and Leu-263 in *Anabaena* FNR with those residues found in NAD<sup>+</sup>/H-dependent members produces an enzyme with a three-dimensional structure having a backbone structure in this region more similar to that shown by NAD<sup>+</sup>/H-dependent members of the FNR family. Therefore, the structure of this mutant explains why it is able to interact more efficiently with NAD<sup>+</sup>/H than both the WT enzyme and the single L263P FNR mutant.

**Effect of Combined Mutations at the 2'-P-AMP and Pyrophosphate Regions of NADP<sup>+</sup>**—In the present study FNR enzymes simultaneously involving several mutations of those residues previously reported as being determinants of coenzyme specificity in *Anabaena* FNR by interacting with the 2'-P group of NADP<sup>+</sup>, Ser-223, Arg-224, Arg-233, and Tyr-235, as well as mutations in the pyrophosphate binding region of NADP<sup>+</sup> described above have been produced and characterized. Analysis of the interaction of these FNR forms with NADP<sup>+</sup> by difference spectroscopy, as well as the  $K_m$  values obtained for NADPH (Table II), clearly indicated that these FNRs, and particularly those containing the S223D mutation, had lost the ability to bind efficiently NADP<sup>+</sup>/H. Consequently, due to the lack of optimal interaction, the efficiency and the rate constants obtained for the reduction of any of these FNR forms by NADPH was considerably lower than those reported for the WT (Table II and Table III). Such behavior was expected for those mutants containing the S223D mutation because, as previously shown (1), the Ser-223 side chain is crucial in determining FNR coenzyme specificity for NADPH. Alternatively, the introduction of a negative charge at this position almost completely prevents the FNR-NADP<sup>+</sup>/H interaction, and it is known that the NAD<sup>+</sup>/H-dependent enzymes of the FNR family possess an Asp residue at the equivalent position (33, 34). Moreover, the combination of mutations at positions Arg-224, Arg-233, and Tyr-235, which had been shown previously to modulate NADP<sup>+</sup> binding to different degrees, produces an important decrease in the ability of FNR to bind NADP<sup>+</sup>. Such behavior must be due to the addition of the effects introduced by the different mutations, which surely modify the geometry of the 2'-P-AMP-binding site and therefore diminish the ability of the various side chains to adapt the site to the nucleotide as has been shown to be necessary for proper NADP<sup>+</sup> binding (16).

With regard to the interaction with NAD<sup>+</sup>, some of these FNR mutants (R224Q/R233L/Y235F and T155G/R224Q/R233L/Y235F) showed weak difference spectra upon addition of this nucleotide, suggesting some interaction with it that is absent in the WT FNR. However, their very high  $K_m$  values for NADH (Table II) indicate a very weak interaction between these mutants and NAD<sup>+</sup>/H. Moreover, no gross improvements are detected for any of these catalytic parameters of the FNR mutant with NADH when compared with those of the WT enzyme (Table II and Table III). Thus, with the only exceptions being the R233L/Y235F, R224Q/R233L/Y235F, and T155G/A160T/S223D/R224Q/R233L/Y235F/L263P FNR mutants that have  $k_{cat}$  and  $k_{app}$  values that are only slightly increased with regard to the WT, most of the FNR forms assayed do not show any improvement in the kinetic constants with NADH (Table II and Table III). Finally, comparison of the steady-state and fast kinetic parameters obtained with both nucleotides, NADPH and NADH, show almost no difference for each FNR form indicating that the combination mutations analyzed produce enzymes that lack the ability to discriminate between

NADP<sup>+</sup>/H and NAD<sup>+</sup>/H. Therefore, our results clearly indicate that replacing several residues at the 2'-P-binding site noticeably reduces the ability of FNR to interact efficiently with NADP<sup>+</sup>/H, and even produces a diminution of the already low affinity of the enzyme for NAD<sup>+</sup>/H. This suggests that precise interaction between a residue of the enzyme in this region in *Anabaena* FNR and the amide ring of NAD(P)<sup>+</sup>/H is required to support efficient complex formation between the protein and the pyridine nucleotide for subsequent hydride transfer.

In summary, our results confirm that the determinants for coenzyme specificity in FNR are not only situated in the 2'-P-binding region but also in the pyrophosphate binding region. Therefore, such conclusion also suggests that other regions of the protein, yet to be identified, might also be involved in this process. Thus, previous studies in the pea enzyme have also shown that replacement by site-directed mutagenesis of the C-terminal tyrosine, Tyr-308 (Tyr-303 in *Anabaena*) produced FNR forms in which the preference for NADP<sup>+</sup>/H over NAD<sup>+</sup>/H was considerably decreased (9). However, these studies suggest that the C-terminal tyrosine enhances the specificity for NADP<sup>+</sup>/H by destabilizing the interaction of the nicotinamide ring of both NADP<sup>+</sup>/H and NAD<sup>+</sup>/H, consequently with Tyr-308 behaving as a negative determinant. Therefore in FNR the determinants of coenzyme specificity must be produced by specific recognition of other regions, such as the 2'-P and pyrophosphate groups of NADP<sup>+</sup>/H, that place the nicotinamide moiety in such a locus to ensure a high degree of discrimination for the coenzyme once the terminal Tyr moves during the catalytic mechanism to allow hydride transfer.

## REFERENCES

- Medina, M., Luquita, A., Tejero, J., Hermoso, J. A., Mayoral, T., Sanz-Aparicio, J., Grever, K., and Gómez-Moreno, C. (2001) *J. Biol. Chem.* **276**, 11902–11912
- Elmore, C. L., and Porter, T. D. (2002) *J. Biol. Chem.* **277**, 48960–48964
- Carrillo, N., and Ceccarelli, E. A. (2003) *Eur. J. Biochem.* **270**, 1900–1915
- Scrutton, N. S., Berry, A., and Perham, R. N. (1990) *Nature* **343**, 38–43
- Chen, R., Greer, A., and Dean, A. M. (1995) *Proc. Natl. Acad. Sci. U. S. A.* **92**, 11666–11670
- Perozich, J., Kuo, I., Wang, B. C., Boesch, J. S., Lindahl, R., and Hempel, J. (2000) *Eur. J. Biochem.* **267**, 6197–6203
- Döhr, O., Paine, M. J. I., Friedberg, T., Roberts, G. C. K., and Wolf, C. R. (2001) *Proc. Natl. Acad. Sci. U. S. A.* **98**, 81–86
- Hurley, J. K., Morales, R., Martínez-Júlvez, M., Brodie, T. B., Medina, M., Gómez-Moreno, C., and Tollin, G. (2002) *Biochim. Biophys. Acta* **1554**, 5–21
- Piubelli, L., Aliverti, A., Arakaki, A. K., Carrillo, N., Ceccarelli, E. A., Karplus, P. A., and Zanetti, G. (2000) *J. Biol. Chem.* **275**, 10472–10476
- Bruns, C. M., and Karplus, P. A. (1995) *J. Mol. Biol.* **247**, 125–145
- Serre, L., Vellieux, F. M. D., Medina, M., Gómez-Moreno, C., Fontecilla-Camps, J. C., and Frey, M. (1996) *J. Mol. Biol.* **263**, 20–39
- Aliverti, A., Deng, Z., Ravasi, D., Piubelli, L., Karplus, P. A., and Zanetti, G. (1998) *J. Biol. Chem.* **273**, 34008–34015
- Deng, Z., Aliverti, A., Zanetti, G., Arakaki, A. K., Ottado, J., Orellano, E. G., Calcaterra, N. B., Ceccarelli, E. A., Carrillo, N., and Karplus, A. (1999) *Nat. Struct. Biol.* **6**, 847–853
- Adak, S., Sharma, M., Meade, A. L., and Stuehr, D. J. (2002) *Proc. Natl. Acad. Sci. U. S. A.* **99**, 13516–13521
- Gutierrez, A., Döhr, O., Paine, M., Wolf, C. R., Scrutton, N. S., and Roberts, G. C. (2000) *Biochemistry* **39**, 15990–15999
- Hermoso, J. A., Mayoral, T., Faro, M., Gómez-Moreno, C., Sanz-Aparicio, J., and Medina, M. (2002) *J. Mol. Biol.* **319**, 1133–1142
- Correll, C. C., Batie, C. J., Ballou, D. P., and Ludwig, M. L. (1992) *Science* **258**, 1604–1610
- Medina, M., Martínez-Júlvez, M., Hurley, J. K., Tollin, G., and Gómez-Moreno, C. (1998) *Biochemistry* **37**, 2715–2728
- Hurley, J. K., Salamon, Z., Meyer, T. E., Fitch, J. C., Cusanovich, M. A., Markley, J. L., Cheng, H., Xia, B., Chae, Y. K., Medina, M., Gómez-Moreno, C., and Tollin, G. (1993) *Biochemistry* **32**, 9346–9354
- Hurley, J. K., Fillat, M. F., Gómez-Moreno, C., and Tollin, G. (1996) *J. Am. Chem. Soc.* **118**, 5526–5531
- Tollin, G. (1995) *J. Bioenerg. Biomembr.* **27**, 303–309
- Leslie, A. G. W. (1987) in *Proceedings of the CCP4 Study Weekend* (Helliwell, J. R., Machin, P. A., and Papiz, M. Z., eds) pp. 39–50, SERC Daresbury Laboratory, Warrington, UK
- Collaborative Computational Project Number 4 (1994) *Acta Crystallogr. Sect. D Biol. Crystallogr.* **50**, 760–763
- Navaza, J. (1994) *Acta Cryst. Sect. A* **50**, 157–163
- Castellano, E., Oliva, G., and Navaza, J. (1992) *J. Appl. Crystallogr.* **25**, 281–284

26. Brünger, A. T. (1993) *X-PLOR: A System for X-ray Crystallography and NMR*, Version 3.851, Yale University Press, New Haven, CT
27. Jones, T. A., Zou, J. Y., Cowan, S. W., and Kjeldgaard, M. (1991) *Acta Crystallogr. Sect. A* **47**, 110–119
28. Pueyo, J. J., and Gómez-Moreno, C. (1991) *Prep. Biochem.* **21**, 191–204
29. Sancho, J., and Gómez-Moreno, C. (1991) *Arch. Biochem. Biophys.* **288**, 231–238
30. Simonsen, R. P., Weber, P. C., Salemme, F. R., and Tollin, G. (1982) *Biochemistry* **24**, 6366–6375
31. Simonsen, R. P., and Tollin, G. (1983) *Biochemistry* **22**, 3008–3016
32. Batie, C. J., and Kamin, H. (1984) *J. Biol. Chem.* **259**, 11976–11985
33. Didierjean, C., Rahuel-Clermont, S., Vitoux, B., Dideberg, O., Branlant, G., and Aubry, A. (1997) *J. Mol. Biol.* **268**, 739–759
34. Holmberg, N., Ryde, U., and Bülow, L. (1999) *Protein Eng.* **12**, 851–856